Phenomenological theory of dynamical light scattering from dielectric bulk waves in semi-infinite opaque crystals

O. Keller
Group of Physics, Institute 7, Aalborg University Centre, DK9100 Aalborg, Denmark
(Received 31 May 1977; revised manuscript received 28 December 1977)

A recently established phenomenological theory of dynamical light scattering from coupled systems of acoustical lattice waves and free-carrier-density waves in unbounded opaque semiconductors has been extended to semi-infinite crystals. On the basis of a quasistatic two-wave interference approximation, expressions have been obtained for the noncollinear real and imaginary parts of the wave vectors of the forward-diffracted optical eigenmodes. The frequency dispersion of the modes, the opacity broadening of the linewidths, the boundary kinematics, and the reflectance have been analyzed. With main emphasis on the plasma dispersion relation in the long-wavelength limit, the basic concepts have been applied to a study of dynamical diffraction from acoustoelectrically bunched conduction electrons in *n*-InSb at 80 K. Numerical results based on a Boltzmann-equation calculation of the free-carrier bunching are presented. A particular analysis is given of the anomalous transmission in the collision-dominated regime ($Ql \ll 1$) of acoustoelectric interaction assuming the electron gas to be collisionless ($\omega\tau \gg 1$) in regard to its optical properties.

I. INTRODUCTION

During the past decade significant progress has been made in our understanding of the processes which are responsible for the inelastic scattering of light by coupled systems of acoustic phonons and free carriers in semiconductors.[1,2]

For crystals in the electronic ground state the coupling of light and sound is macroscopically described by (i) the direct photoelastic effect composed of Pöckels' contribution[3–5] and the rotational contribution,[6] and (ii) the indirect photoelastic effect, that is, the succession of the piezoelectric and electro-optic effects.[7,8] The microscopic formulation of the light-scattering process,[9] which must be applied when studying resonance scattering effects with near-band-gap light, is essentially based on a perturbation-theory description where a photon incident on the crystal in its ground state creates a virtual electron-hole pair. The electron or hole then interacts with a phonon via the deformation-potential coupling or the piezoelectric coupling, and subsequently recombines emitting the scattered photon. In extended theories of resonant Brillouin scattering[10,11] the strongly coupled systems of photons and quasilocalized electron-hole pairs are treated as exciton polaritons, and the scattering of polaritons[12] by acoustic phonons is considered.

When the conduction band is partially filled the free-carrier screening of the indirect photoelastic effect must be taken into account.[1,13,14] For nonthermal phonon distributions this has been done on the basis of a Boltzmann-equation calculation of the phonon-induced self-consistent field arising from the piezoelectric coupling and the deformation-potential coupling.[15,16]

The free carriers also scatter light directly, either as single particles or as collective plasmons.[1,17] If the conduction electrons are strongly bunched, as they can be in the potential wells of an acoustoelectric domain, the inelastic scattering from this non-equilibrium free-carrier density modulation can be comparable in magnitude with the scattering from the lattice.[18,19]

Historically, inelastic-light-scattering investigations have been confined to transparent media. At the moment, however, the studies are being extended to photon energies above the band gap[1] and below the plasma edge.[20] When the crystal is opaque to the incident and scattered light the pseudomomentum conservation law breaks down and the inelastic scattering becomes possible with excitations within a range of wave vectors.[1,21,22] Furthermore, interference effects among the incoming and scattered beams must be considered. This can be done by replacing the usual kinematical theory of diffraction by a dynamical one.[20] Using a phenomenological dynamical model it has been predicted[20] that one can obtain sound-induced anomalous transmission of light below the plasma edge in piezoelectric semiconductors, an effect which to some extent is analogous to the Borrmann effect[23] known from γ-ray,[24] x-ray,[23,25–28] neutron,[29] and electron diffraction.[30]

The purpose of this paper is, on the basis of a

two-wave interference approximation, (i) to formulate a phenomenological theory of dynamical light diffraction from a quasistatic fluctuation in the complex optical dielectric tensor of a semi-infinite conducting crystal, (ii) to determine the boundary transfer functions, (iii) to study the frequency dispersion relations of the optical eigenmodes, (iv) to consider the opacity broadening of the linewidths of the forward diffracted modes, (v) to apply the general formulation to a study of dynamical diffraction from acoustoelectrically bunched conduction electrons in InSb, and finally (vi) to discuss the diffraction in the limit where the solid-state plasma is collisionless ($\omega\tau >> 1$).

II. BOUNDARY KINEMATICS

In this section the reflection and transmission kinematics of a plane electromagnetic wave impinging from vacuum on a plane boundary of a semi-infinite electrically conducting crystal is determined. It is required that the interaction of the transmitted wave with a selected plane-wave component of the propagating dielectric disturbance is phase matched. Furthermore, it is assumed that the dielectric excitation travels parallel to the surface, and that the scattering plane inside and the plane of incidence outside the crystal are parallel.

In complex notation the electric fields of the incident (i) and reflected (r) optical waves are described as follow:

$$\vec{E}_\alpha(\vec{r},t) = \vec{E}_{\vec{k}_\alpha} \exp[i(\vec{k}_\alpha \cdot \vec{r} - \omega_\alpha t)] \ , \quad \alpha = i,r \ , \quad (1)$$

where $\vec{E}_{\vec{k}_\alpha}$ is the complex amplitude of the mode, $\vec{k}_\alpha$ is the wave vector, which is real in vacuum, and ω_α is the angular frequency. By assuming that the time-averaged intensity of the incoming wave does not change in time, ω_i is a real quantity. The electric fields of the transmitted (t) and the Raman scattered (s) waves, which are traveling through an absorbing medium, are written on the form

$$\vec{E}_\beta(\vec{r},t) = \vec{E}_{\vec{k}_\beta} \exp[i(\vec{k}_\beta \cdot \vec{r} - \omega_\beta t) - \vec{\gamma}_\beta \cdot \vec{r}] \ , \quad \beta = t,s \ , \quad (2)$$

where the complex wave vector of the mode has been splitted into a real part $\vec{k}_\beta$, determining the wavelength, and an imaginary part $\vec{\gamma}_\beta$, characterizing the amplitude attenuation phenomenologically.

Continuity of the tangential component of the electric field across the boundary implies that (i) the components of the real parts of the incident, reflected and transmitted wave vectors along the surface are equal, i.e.,

$$\vec{k}_i \cdot \hat{\kappa} = \vec{k}_r \cdot \hat{\kappa} = \vec{k}_t \cdot \hat{\kappa} \ , \quad (3)$$

where $\hat{\kappa}$ is a unit vector parallel to the intersection line between the scattering plane and the boundary plane, and that (ii) the planes of constant amplitude are parallel to the boundary, i.e.,

$$\vec{\gamma}_t = \gamma_t \hat{n} \ , \quad (4)$$

where $\hat{n}$ is a unit vector perpendicular to the surface. Note that the four vectors $\vec{k}_i$, $\vec{k}_r$, $\vec{k}_t$, and $\vec{\gamma}_t$ are coplanar.

In the following we consider a phase matched interaction of the transmitted wave with a plane-wave component

$$\vec{\epsilon}(\vec{r},t) = \vec{\epsilon}_{\vec{Q}} \exp[i(\vec{Q} \cdot \vec{r} - \Omega_{\vec{Q}} t)] \ , \quad (5)$$

of the linear part of the relative complex dielectric tensor at optical frequencies. The unperturbed relative dielectric tensor will be denoted by $\vec{\epsilon}_0$. Since we shall be dealing with bulk waves only it is assumed that the Fourier amplitude $\vec{\epsilon}_{\vec{Q}}$ is independent of the depth below the crystal surface. In a forthcoming paper an investigation of the possibilities for anomalous electromagnetic penetration below the plasma edge in metals by modulating the free-carrier density of the surface via coupling to acoustic surface waves will be undertaken. For dielectric modes undamped in space and time, the wave vector $\vec{Q}$ and the angular frequency $\Omega_{\vec{Q}}$ are real quantities. Note that the unessential restriction $\vec{Q} = Q\hat{\kappa}$ is imposed on the analysis.

Phase matching in a first-order Stokes (minus sign) or anti-Stokes (plus sign) scattering process requires that the real and imaginary part of the wave vector of the scattered field must fulfil the conditions

$$\vec{k}_s = \vec{k}_t \pm \vec{Q} \ , \quad (6)$$

and

$$\vec{\gamma}_s = \gamma_s \hat{n} \ . \quad (7)$$

Energy conservation in the inelastic scattering event implies that $\omega_s = \omega_t \pm \Omega_{\vec{Q}}$. However, since only low-frequency excitations ($\Omega_{\vec{Q}} << \omega_i$) are of interest in this work, we shall in the following sections neglect the Doppler shifts. The angular frequency of light will be denoted by ω.

The ratio of the magnitudes of the real parts of the optical wave vectors involved in the scattering process is given by

$$\frac{k_s}{k_t} = \frac{n_s(\omega_s, \vec{k}_s)}{n_t(\omega_t, \vec{k}_t)} \left\{ 1 \pm \frac{\Omega_{\vec{Q}}}{\omega_t} \right\} \ , \quad (8)$$

where n_t and n_s are the refractive indices of the two waves. Deviations of the above ratio from unity gives rise to optically anisotropy effects in the scattering geometry. Here we shall neglect such effects arising from the inelasticity of the collision "directly" [last factor in Eq. (8)],[31] the frequency dispersion,[1] and

the angular dispersion[32] of the refractive index. Thus, the treatment is limited to cases where $\hat{\kappa}$ is parallel to one of the principal dielectric axes of the crystal, and where there is no change of light polarization in the scattering process. With these restrictions one has $|\vec{k}_s| = |\vec{k}_t|$ and $|\vec{\gamma}_s| = |\vec{\gamma}_t|$.

In the isotropic scattering configuration the wave vector of the reflected light is given by

$$\vec{k}_r = -(\vec{k}_i \pm \vec{Q}) \ . \tag{9}$$

III. WAVE FIELD IN TWO-WAVE INTERFERENCE APPROXIMATION

To determine the electromagnetic field inside the crystal in the limit of quasielastic scattering one has to solve the time-independent wave equation

$$\left[\vec{\nabla}\vec{\nabla} - \vec{1}\nabla^2 - \left(\frac{\omega}{c}\right)^2 [\vec{\epsilon}_0 + \vec{\epsilon}(\vec{r},\omega)]\right] \cdot \vec{E}(\vec{r},\omega) = 0 \ , \tag{10}$$

where $\vec{\nabla}$ is the gradient operator, and $\vec{1}$ is the unit tensor. Restricting ourselves to the important case where the incident and scattered waves are polarized perpendicular to the scattering plane, the electric field can, in a two-wave interference approximation be written on the form

$$\vec{E}(\vec{r},\omega) = \hat{n} \times \hat{\kappa}[E_t(\hat{n}\cdot\vec{r}) \exp(i\vec{k}_t \cdot \hat{\kappa}\,\hat{\kappa}\cdot\vec{r}) + E_s(\hat{n}\cdot\vec{r}) \exp(i\vec{k}_s \cdot \hat{\kappa}\,\hat{\kappa}\cdot\vec{r})] \ , \tag{11}$$

where it has been indicated explicitly that the complex amplitudes E_t and E_s are functions of the distance from the surface only. Combining Eqs. (5) and (6) on isotropic form, (10) and (11) one obtains the following coupled differential equations for determining E_t and E_s

$$\frac{d^2E_t(x)}{dx^2} + \left[\left(\frac{\omega}{c}\right)^2 \tilde{\epsilon}_0 - \frac{Q^2}{4}\right] E_t(x) + \left(\frac{\omega}{c}\right)^2 \tilde{\epsilon}_{\vec{Q}}{}^* E_s(x) = 0 \ , \tag{12}$$

and

$$\frac{d^2E_s(x)}{dx^2} + \left[\left(\frac{\omega}{c}\right)^2 \tilde{\epsilon}_0 - \frac{Q^2}{4}\right] E_s(x) + \left(\frac{\omega}{c}\right)^2 \tilde{\epsilon}_{\vec{Q}} E_t(x) = 0 \ , \tag{13}$$

where $\tilde{\epsilon}_0$ and $\tilde{\epsilon}_{\vec{Q}}$ denote the appropriate components of the dielectric tensor. In addition we have introduced $x = \hat{n}\cdot\vec{r}$, and utilized that $\tilde{\epsilon}_{-\vec{Q}} = \tilde{\epsilon}_{\vec{Q}}{}^*$. As a trial solution to Eqs. (12) and (13) plane waves of the form $E_t(x) = E_{\vec{k}_t} \exp[(ik-\gamma)x]$ and $E_s(x) = E_{\vec{k}_s} \times \exp[(ik-\gamma)x]$ with $k = \vec{k}_t \cdot \hat{n} = \vec{k}_s \cdot \hat{n}$, are taken. The condition that the determinant of the algebraic equations in $E_{\vec{k}_t}$ and $E_{\vec{k}_s}$ must equal zero implies that

$$(k+i\gamma)^2 = -\frac{Q^2}{4} + \left(\frac{\omega}{c}\right)^2 (\tilde{\epsilon}_0 \pm |\tilde{\epsilon}_{\vec{Q}}|) \ . \tag{14}$$

By solving Eq. (14) one finds that the two eigenvalues $(+,-)$ of the wave vector components perpendicular to the surface are given by

$$k^{\pm} = \frac{\omega}{c}\left[\frac{1}{2}\left(\left\{\left[\mathrm{Re}\tilde{\epsilon}_0 \pm |\tilde{\epsilon}_{\vec{Q}}| - \left(\frac{Qc}{2\omega}\right)^2\right]^2 + (\mathrm{Im}\tilde{\epsilon}_0)^2\right\}^{1/2} + \mathrm{Re}\tilde{\epsilon}_0 \pm |\tilde{\epsilon}_{\vec{Q}}| - \left(\frac{Qc}{2\omega}\right)^2\right)\right]^{1/2} \ , \tag{15}$$

and

$$\gamma^{\pm} = \frac{\omega}{c}\left[\frac{1}{2}\left(\left\{\left[\mathrm{Re}\tilde{\epsilon}_0 \pm |\tilde{\epsilon}_{\vec{Q}}| - \left(\frac{Qc}{2\omega}\right)^2\right]^2 + (\mathrm{Im}\tilde{\epsilon}_0)^2\right\}^{1/2} - \mathrm{Re}\tilde{\epsilon}_0 \mp |\tilde{\epsilon}_{\vec{Q}}| + \left(\frac{Qc}{2\omega}\right)^2\right)\right]^{1/2} \ , \tag{16}$$

in a dynamical approach to light diffraction in a semi-infinite crystal. The quantities $\mathrm{Re}\tilde{\epsilon}_0$ and $\mathrm{Im}\tilde{\epsilon}_0$ denote the real and imaginary part of $\tilde{\epsilon}_0$. The wave-vector components of the plus and minus sign modes parallel to the boundary are equal, and in magnitude given by $|\vec{k}_t \cdot \hat{\kappa}| = |\vec{k}_s \cdot \hat{\kappa}| = Q/2 = \Omega_{\vec{Q}}/(2V_p)$, where V_p is the phase velocity of the dielectric wave. The quasielastic dynamical diffraction kinematics of the two eigenmodes and the boundary kinematics are shown schematically in Fig. 1.

The result obtained in Eqs. (15) and (16) deviate slightly from that found previously[20] for an unbounded medium. This is due to the fact that it was assumed there that the real and imaginary part of the optical wave vector were collinear, whereas in this work we are dealing with inhomogeneous waves.

For $Q \to 0$ and $|\tilde{\epsilon}_{\vec{Q}}| \to 0$ Eqs. (15) and (16) are reduced to the well-known expressions for unperturbed wave propagation at normal incidence in opaque media. Note that the propagation constants of a dielectric perturbed crystal can be obtained from the unperturbed case by making the replacement

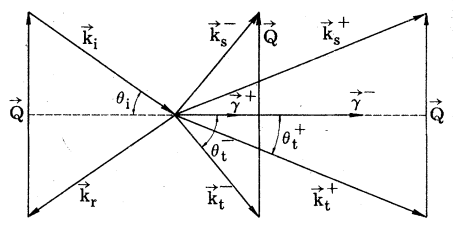

FIG. 1. Schematic diagram showing the quasielastic dynamical diffraction kinematics for the two inhomogeneous optical eigenmodes in an isotropic scattering configuration.

$$\mathrm{Re}\tilde{\epsilon}_0 \rightarrow \mathrm{Re}\tilde{\epsilon}_0 \pm |\tilde{\epsilon}_{\vec{Q}}| - \left(\frac{Qc}{2\omega}\right)^2 . \tag{17}$$

According to Eq. (16) the condition for high transparency of the crystal is

$$0 < \frac{|\mathrm{Im}\tilde{\epsilon}_0|}{\mathrm{Re}\tilde{\epsilon}_0 \pm |\tilde{\epsilon}_{\vec{Q}}| - \left(\frac{Qc}{2\omega}\right)^2} \ll 1 , \tag{18}$$

in a two-wave interference approximation. A phenomenological determination of the frequency regions of induced anomalous transmission of light through absorbing crystals is accomplished by comparing Eq. (18) with the condition

$$0 < \frac{|\mathrm{Im}\tilde{\epsilon}_0|}{\mathrm{Re}\tilde{\epsilon}_0} \ll 1 , \tag{19}$$

for high transparency in dielectric undisturbed media.

The field eigenvectors corresponding to the wave vector eigenvalues obtained in Eqs. (15) and (16) are related by a phase factor $\phi_{\vec{Q}}$ given by

$$\frac{E^{\pm}_{\vec{k}_s}}{E^{\pm}_{\vec{k}_t}} = \pm e^{i\phi_{\vec{Q}}} , \quad \tan\phi_{\vec{Q}} = \frac{\mathrm{Im}\tilde{\epsilon}_{\vec{Q}}}{\mathrm{Re}\tilde{\epsilon}_{\vec{Q}}} , \tag{20}$$

for the anti-Stokes process. For the Stokes event the phase factor is $\phi_{-\vec{Q}} = -\phi_{\vec{Q}}$.

The solution of the system of coupled differential equations (12) and (13), which satisfies the boundary condition $E_t(x=0) = T_\perp E_{\vec{k}_i}$, $T_\perp$ being the amplitude reflection coefficient for light polarized perpendicular to the plane of incidence, and $E_s(x=0) = 0$ at the surface, and the condition $E_t(x \rightarrow \infty) = E_s(x \rightarrow \infty) = 0$ at infinity, takes the form

$$E_t(x) = \frac{T_\perp}{2} E_{\vec{k}_i} \{\exp[(ik^+ - \gamma^+)x] + \exp[(ik^- - \gamma^-)x]\} , \tag{21}$$

and

$$E_s(x) = \frac{T_\perp}{2} E_{\vec{k}_i} \{\exp[(ik^+ - \gamma^+)x] - \exp[(ik^- - \gamma^-)x]\} \exp(i\phi_{\vec{Q}}) , \tag{22}$$

or in short notation $E_t = E_t^+ + E_t^-$ and $E_s = (E_t^+ - E_t^-)\exp(i\phi_{\vec{Q}})$.

By combining Eqs. (6), (11), (21), and (22) it follows immediately that the total wave field in complex notation is given by

$$\vec{E}(\vec{r},t) = T_\perp E_{\vec{k}_i} \hat{n} \times \hat{\kappa} \exp(i\phi_{\vec{Q}}/2) \times \left\{ \exp[i(k^+\hat{n}\cdot\vec{r} - \omega t) - \gamma^+\hat{n}\cdot\vec{r}] \cos\left(\frac{Q}{2}\hat{\kappa}\cdot\vec{r} + \frac{\phi_{\vec{Q}}}{2}\right) + \exp\left[i\left(k^-\hat{n}\cdot\vec{r} - \omega t - \frac{\pi}{2}\right) - \gamma^-\hat{n}\cdot\vec{r}\right] \sin\left(\frac{Q}{2}\hat{\kappa}\cdot\vec{r} + \frac{\phi_{\vec{Q}}}{2}\right) \right\} . \tag{23}$$

The interpretation of Eq. (23) is quite obvious and similar to that given previously[20] for an infinite medium. The field consists of two components propagating with phase velocities ω/k^+ and ω/k^- perpendicular to the boundary. The amplitude attenuation coefficients of the modes are γ^+ and γ^-, respectively. The travelling waves differ in phase by the amount $\pi/2$ at the surface. Parallel to the boundary the wave pattern for each of the two modes is standing. The phase shift between the two patterns is $\pi/2$.

IV. BOUNDARY TRANSFER FUNCTIONS

In this section the amplitude reflection and transmission coefficients of the electric field at the interface between vacuum and an absorbing crystal where the optical dielectric constant exhibits a sinusoidal spatial modulation are evaluated. It is assumed that the bulk modulation determines the reflectance and the refractivity, that the boundary kinematics is appropriate for quasielastic Bragg scattering in the crystal, and that the electric field is polarized parallel to the boundary plane (TE geometry).

In the two-wave interference approximation to dynamical diffraction the boundary conditions giving the continuity of the tangential components of the electric and magnetic field at $x=0$ are $E_i + E_t = E_t^+ + E_t^-$, and $(\omega/c)(E_i - E_t)\cos\theta_i = (k^+ + i\gamma^+)E_t^+ + (k^- + i\gamma^-)E_t^-$, where θ_i is the Bragg angle outside the crystal. Since $E_t^+ = E_t^- = E_t/2 = (T_\perp/2)E_{\vec{k}_i}$ at the surface our elementary considerations show that the amplitude reflection coefficient is given by

$$R_\perp = \frac{\left[\left(\frac{\omega}{c}\right)^2 - \left(\frac{Q}{2}\right)^2\right]^{1/2} - \frac{1}{2}(k^+ + k^-) - \frac{i}{2}(\gamma^+ + \gamma^-)}{\left[\left(\frac{\omega}{c}\right)^2 - \left(\frac{Q}{2}\right)^2\right]^{1/2} + \frac{1}{2}(k^+ + k^-) + \frac{i}{2}(\gamma^+ + \gamma^-)} , \tag{24}$$

and the amplitude transmission coefficient as

$$T_\perp = \frac{\left[\left(\frac{2\omega}{c}\right)^2 - Q^2\right]^{1/2}}{\left[\left(\frac{\omega}{c}\right)^2 - \left(\frac{Q}{2}\right)^2\right]^{1/2} + \frac{1}{2}(k^+ + k^-) + \frac{i}{2}(\gamma^+ + \gamma^-)} \quad . \tag{25}$$

It follows from Eqs. (15), (16), and (24) that measurements of the reflectivity in principle enable one to obtain the Fourier amplitude $|\tilde{\epsilon}_{\vec{Q}}|$ of the dielectric excitation.

The formulas for $R_\perp$ and $T_\perp$ can be obtained from the corresponding equations for a translational invariant medium if (i) the component of the complex wave vector perpendicular to the boundary plane is replaced by the arithmetical mean value $[(k^+ + k^-) + i(\gamma^+ + \gamma^-)]/2$, and (ii) the angle of incidence is chosen in accordance with the appropriate Bragg interference condition.

The forward diffracted eigenmodes are characterized by the complex refractive indices $n^\pm = c(k^\pm + i\gamma^\pm)/\omega$.

In the limit of vanishing dielectric perturbation, i.e., for $Q \to 0$, $k^\pm \to k$, and $\gamma^\pm \to \gamma$, Eqs. (24) and (25) are reduced to the well known expressions for the amplitude reflection and transmission coefficients for perpendicular incidence on an absorbing crystal.

It should be noticed that Snell's law for an absorbing, periodic structure takes the generalized form

$$\sin\theta_i = \left[(\mathrm{Re}\, n^\pm)^2 + \left(\frac{cQ}{2\omega}\right)^2\right]^{1/2} \sin\theta_t^\pm \quad , \tag{26}$$

where $\theta_t^\pm$ are the angles of refraction for the eigenmodes. Snell's law for the unperturbed case is obtained in the limit $Q \to 0$ and $|\tilde{\epsilon}_{\vec{Q}}| \to 0$.

V. DISPERSION RELATION OF FORWARD-DIFFRACTED EIGENMODES

It is obvious from Eq. (15) that the two forward-diffracted eigenmodes are subjected to a frequency dispersion that differs substantially from that of an electromagnetic wave in an unperturbed conducting crystal. A qualitative study of the dispersion can be achieved by comparing the magnitudes of the group velocity $W_g^\pm = \partial\omega/\partial k^\pm$ and the phase velocity $W_p^\pm = \omega/k^\pm$ of the optical modes.

Defining a two-dimensional vector

$$\vec{\mathcal{E}}^\pm = (\mathcal{E}_1^\pm, \mathcal{E}_2) = \left(\mathrm{Re}\tilde{\epsilon}_0 \pm |\tilde{\epsilon}_{\vec{Q}}| - \left(\frac{Qc}{2\omega}\right)^2, \mathrm{Im}\tilde{\epsilon}_0\right) \quad , \tag{27}$$

of which the first component only depends on the dielectric modulation, the frequency dispersion can be expressed in compact notation as follows

$$W_g^\pm = W_p^\pm \left[1 + \left(\frac{W_p^\pm}{2c}\right)^2 \left(\frac{\partial \mathcal{E}_1^\pm}{\partial \ln\omega} + \hat{E}^\pm \cdot \frac{\partial \vec{\mathcal{E}}^\pm}{\partial \ln\omega}\right)\right]^{-1} \quad , \tag{28}$$

where $\hat{\mathcal{E}}^\pm = \vec{\mathcal{E}}^\pm / \mathcal{E}^\pm$.

In the limit $\mathrm{Im}\tilde{\epsilon}_0 \to 0$, the deviation between the group and phase velocities becomes on normalized form

$$\frac{W_p^\pm - W_g^\pm}{W_g^\pm} = \frac{\omega \frac{\partial \mathcal{E}_1^\pm}{\partial\omega}}{|\mathcal{E}_1^\pm| + \mathcal{E}_1^\pm} \quad . \tag{29}$$

In the discussion of anomalous wave propagation in a collisionless solid-state plasma (see Sec. VII) explicit use is made of Eq. (29).

VI. OPACITY BROADENING OF LINEWIDTHS

In opaque crystals a broadening of the linewidths of the forward-diffracted modes can occur in excess of other broadening mechanisms. The broadening is determined by the distribution of wave vectors which is obtained by a Fourier transform of the exponentially absorbed eigenmodes. Opacity broadening effects somewhat similar to those predicted below in connection with dynamical diffraction have been discussed and observed in Raman and Brillouin scattering studies on metals and semiconductors.[1,21,22,33,34]

The squared amplitudes of the spatial Fourier components (denoted by the scalar index q) of the forward diffracted field given in Eq. (23) are

$$|\vec{E}_q| = |T_\perp E_{\vec{k}_i}|^2 \left[C^+(q) + C^-(q) + \frac{4C^+(q)C^-(q)}{\sin 2\delta} \times [\gamma^-(k^+ - q) - \gamma^+(k^- - q)]\right] \quad , \tag{30}$$

where the unnormalized Fourier spectrum of each of the modes in absence of the other ($\delta = 0, \pi/2$) takes the Lorentzian form

$$C^\pm(q) = [(k^\pm - q)^2 + (\gamma^\pm)^2]^{-1} \times \begin{cases} \cos^2\delta \\ \sin^2\delta \end{cases} \quad , \tag{31}$$

with $\delta = (Q/2)\hat{\kappa}\cdot\vec{r} + \phi_{\vec{Q}}/2$.

If the conditions

$$\mathrm{Re}\tilde{\epsilon}_0 - \left(\frac{Qc}{2\omega}\right)^2 >> |\tilde{\epsilon}_{\vec{Q}}| >> |\mathrm{Im}\tilde{\epsilon}_0| \quad , \tag{32}$$

are fulfilled the modes are well-separated ($|k^+ - k^-| >> |\gamma^+| + |\gamma^-|$) and suffer weak absorption only ($k^\pm >> |\gamma^\pm|$), so that one can neglect the

interference term in Eq. (30). The conditions in Eq. (32) lead to the separately normalized (N) Lorentzian spectra

$$C_N^{\pm}(q) \simeq \frac{k^0\gamma^0}{\pi} \frac{k^{\pm}}{(k^{\pm})^2(k^{\pm}-q)^2+(k^0\gamma^0)^2} \quad , \quad (33)$$

if one uses the important general relations

$$k^{\pm}\gamma^{\pm} = k^0\gamma^0 \quad , \quad (34)$$

which are obtained by combining Eqs. (15) and (16). The index 0 on the propagation constants refer to the dielectric unperturbed case. Also in the case where one mode is strongly damped Eq. (33) approximates the spectrum of the other.

The wave-vector spread causes frequency broadenings

$$\Delta\omega^{\pm} \simeq \gamma^{\pm} W_g^{\pm} \quad , \quad (35)$$

in the perturbed opaque crystal. The ratios between these linewidths broadenings and that obtained in an unperturbed absorbing crystal are given by

$$\frac{\Delta\omega^{\pm}}{\Delta\omega^0} \simeq \frac{W_g^{\pm} W_p^{\pm}}{W_g^0 W_p^0} \quad . \quad (36)$$

VII. DYNAMICAL DIFFRACTION IN A BUNCHED COLLISIONLESS PLASMA

In this section the dynamical diffraction from a nonthermal free-carrier-density wave in a collisionless solid-state plasma[17,35] is considered. The two-wave interference approximation is adopted, and it is assumed that the scattering from the plasma dominates.[13,15,16,18,19]

For a parabolic band structure the appropriate dielectric constant is given by

$$\tilde{\epsilon}_0 = \tilde{\epsilon}_0^L \left[1 - \left(\frac{\tilde{\omega}_p}{\omega}\right)^2\right] \quad , \quad (37)$$

in the long-wavelength limit.[20,36] The lattice contribution to the dielectric constant is denoted by $\tilde{\epsilon}_0^L$ and the appropriate plasma frequency by $\tilde{\omega}_p$. Assuming $\tilde{\epsilon}_0^L$ to be real[15,16] it follows that $\mathrm{Im}\tilde{\epsilon}_0 = 0$. Naming the ratio between the considered Fourier amplitude of the space charge-density wave and the thermal equilibrium density by $\tilde{\Delta}_{\vec{Q}}$, the perturbation of the dielectric constant can be written[13,15,16]

$$\tilde{\epsilon}_{\vec{Q}} = -\tilde{\epsilon}_0^L \left(\frac{\tilde{\omega}_p}{\omega}\right)^2 \tilde{\Delta}_{\vec{Q}} \quad . \quad (38)$$

By inserting Eqs. (37) and (38) into (18) one finds that the crystal becomes highly transparent for the forward diffracted beams at frequencies

$$\omega \geqslant \tilde{\omega}_{\mathrm{dyn}}^{\pm} = \left[\tilde{\omega}_p^2(1 \mp |\tilde{\Delta}_{\vec{Q}}|) + \left(\frac{Qc}{2(\tilde{\epsilon}_0^L)^{1/2}}\right)^2\right]^{1/2} \quad , \quad (39)$$

if one neglects the frequency dispersion of $\tilde{\epsilon}_0^L$. In a forthcoming paper we shall investigate the dynamical diffraction of phonon-polaritons in a plasma (i.e., plasmaritons in the limiting case of zero magnetic field) by free-carrier-density waves.

The angular frequencies $\tilde{\omega}_{\mathrm{dyn}}^{\pm}$ given above can be considered as plasma frequencies for the eigenmodes of dynamical diffraction in a plasma perturbed by a quasistatic sinusoidal disturbance.

Combining Eqs. (15), (16), (37), and (38) one obtains in the region $\omega \geqslant \tilde{\omega}_{\mathrm{dyn}}^{\pm}$ the following expressions for the propagation constants

$$k^{\pm} = \frac{\tilde{\omega}_p}{c/(\tilde{\epsilon}_0^L)^{1/2}} \left[\left(\frac{\omega}{\tilde{\omega}_p}\right)^2 - 1 \pm |\tilde{\Delta}_{\vec{Q}}| - \left(\frac{c/(\tilde{\epsilon}_0^L)^{1/2}}{2V_p}\right)^2 \left(\frac{\Omega_{\vec{Q}}}{\tilde{\omega}_p}\right)^2\right]^{1/2} \quad , \quad (40)$$

and

$$\gamma^{\pm} = 0 \quad . \quad (41)$$

In the frequency range $\omega \leqslant \tilde{\omega}_{\mathrm{dyn}}^{\pm}$ absorption characterized by

$$k^{\pm} = 0 \quad , \quad (42)$$

and

$$\gamma^{\pm} = \frac{\tilde{\omega}_p}{c/(\tilde{\epsilon}_0^L)^{1/2}} \left[1 \mp |\tilde{\Delta}_{\vec{Q}}| - \left(\frac{\omega}{\tilde{\omega}_p}\right)^2 + \left(\frac{c/(\tilde{\epsilon}_0^L)^{1/2}}{2V_p}\right)^2 \left(\frac{\Omega_{\vec{Q}}}{\tilde{\omega}_p}\right)^2\right]^{1/2} \quad , \quad (43)$$

takes place.

The presence of the space-charge wave causes a splitting of the plasma dispersion relation into two branches as shown schematically in Fig. 2. It appears from Eq. (40) that the eigenfrequencies at zero wave vector are related to the free-carrier-density modulation by

$$(\tilde{\omega}_{\mathrm{dyn}}^{-})^2 - (\tilde{\omega}_{\mathrm{dyn}}^{+})^2 = 2|\tilde{\Delta}_{\vec{Q}}|\tilde{\omega}_p^2 \quad . \quad (44)$$

This means that the splitting opens up a possibility for measuring the amplitude of the space-charge wave.

Since one always has $\tilde{\omega}_p < \tilde{\omega}_{\mathrm{dyn}}^{-}$ it follows that the minus-sign mode in comparison to the unperturbed wave suffers enhanced absorption and has a higher cutoff frequency.

For the plus-sign mode one obtains the cutoff below the plasma edge, i.e., $\tilde{\omega}_{\mathrm{dyn}}^{+} < \tilde{\omega}_p$, if the condition

$$|\tilde{\Delta}_{\vec{Q}}| > \left(\frac{c/(\tilde{\epsilon}_0^L)^{1/2}}{2V_p}\right)^2 \left(\frac{\Omega_{\vec{Q}}}{\tilde{\omega}_p}\right)^2 \quad , \quad (45)$$

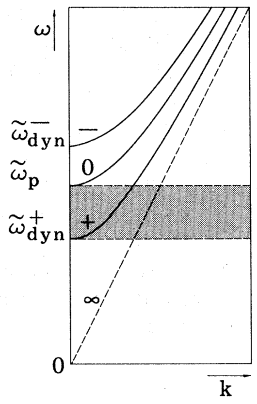

FIG. 2. Dispersion relations for dynamically diffracted (+, −) and undiffracted (0) electromagnetic eigenmodes of long wavelength in a collisionless solid-state plasma. Neglecting band-structure effects the curves approach a common nondispersive $\omega(\vec{k})$ relation (∞) at high frequencies. In the shaded region anomalous transmission takes place for the plus-sign mode.

is fulfilled. Introducing the optical wave vector $\tilde{k}_p$, corresponding to the frequency $\tilde{\omega}_p$ in an insulating crystal, i.e., $\tilde{k}_p = \tilde{\omega}_p/[c/(\tilde{\epsilon}_0^L)^{1/2}]$ the inequality (45) can be written alternatively as

$$|\tilde{\Delta}_{\vec{Q}}| > \sin^2\theta_t(\omega=\tilde{\omega}_p, \tilde{\Delta}_{\vec{Q}}=0) = \left(\frac{Q}{2\tilde{k}_p}\right)^2 , \quad (46)$$

where $\theta_t(\omega=\tilde{\omega}_p, \tilde{\Delta}_{\vec{Q}}=0)$ is the Bragg angle obtained inside the crystal if the conduction electrons were removed and the frequency of the incident radiation was equal to the plasma frequency.

It should be noticed that the factor $[c/(\tilde{\epsilon}_0^L)^{1/2}]/2V_p$ for a specific polarization of the disturbance varies only little from one material to another.

If $\omega < \tilde{\omega}^+_{dyn}$ both eigenmodes are strongly damped, if $\tilde{\omega}^+_{dyn} < \omega < \tilde{\omega}^-_{dyn}$ nearly free propagation takes place for the plus sign mode, and finally if $\omega > \omega^-_{dyn}$ both eigenmodes travel almost undamped.

Utilizing Eq. (29) one obtains for the group velocities the result

$$W_g^{\pm} = \frac{c}{(\tilde{\epsilon}_0^L)^{1/2}}\left[1-\left(\frac{\tilde{\omega}^{\pm}_{dyn}}{\omega}\right)^2\right]^{1/2} , \quad \omega > \tilde{\omega}^{\pm}_{dyn} . \quad (47)$$

The group and phase velocities of the modes are linked via the simple relation

$$W_g^{\pm} W_p^{\pm} = W_g^0 W_p^0 \left[= \left(\frac{c}{(\tilde{\epsilon}_0^L)^{1/2}}\right)^2\right] . \quad (48)$$

The second equality in Eq. (48) is recognized from elementary analysis of electromagnetic wave propagation in homogeneous plasmas.

The reflectance $|R_\perp|^2$, can be calculated by inserting Eqs. (40)–(43) in (24). When $\omega < \tilde{\omega}^+_{dyn}$, is $k^{\pm}=0$ so that

$$|R_\perp|^2 \simeq 1 , \quad \omega < \tilde{\omega}^+_{dyn} . \quad (49)$$

For $\tilde{\omega}^+_{dyn} < \omega < \tilde{\omega}^-_{dyn}$, one has $k^-=0$ and $\gamma^+=0$, implying that

$$|R_\perp|^2 \simeq 1 - \frac{2B^+}{(1+B^+)\left[1-\left(\frac{Qc}{2\omega}\right)^2\right] + \frac{1}{2}\tilde{\epsilon}_0^L\left(\frac{\tilde{\omega}_p}{\omega}\right)^2 |\tilde{\Delta}_{\vec{Q}}|} ,$$

$$\tilde{\omega}^+_{dyn} < \omega < \tilde{\omega}^-_{dyn} , \quad (50)$$

where $B^{\pm} = k^{\pm}/\vec{k}_i \cdot \hat{n}$ is defined as the ratio between the wave numbers perpendicular to the boundary inside and outside the medium. When $\tilde{\omega}^-_{dyn} < \omega$, one finds $\gamma^{\pm}=0$. This shows that $R_\perp$ is real and that

$$|R_\perp|^2 \simeq \left(\frac{2-B^+-B^-}{2+B^++B^-}\right)^2 , \quad \tilde{\omega}^-_{dyn} < \omega \quad (51)$$

It appears from Eqs. (49)–(51) that it should be possible to determine in principle the free-carrier- density modulation and consequently $k^{\pm}$ and $\gamma^{\pm}$ by analyzing the reflectance.

VIII. DYNAMICAL DIFFRACTION FROM ACOUSTOELECTRICALLY BUNCHED CONDUCTION ELECTRONS IN *n*-InSb

In the following the formal considerations outlined in Sec. II–IV are applied to a quantitative study of dynamical diffraction of light from a nonthermal free-carrier-density wave in *n*-InSb generated by acoustoelectric interaction of conduction electrons and piezoelectrically active sound waves.

A. Quasistatic perturbation of the dielectric constant

Let us consider a piezoelectrically active shear wave propagating along a [110] direction in a *n*-InSb crystal (possessing the cubic zinc blende structure), and with ionic displacement in the [001] direction. The phase velocity of this pure TA mode is given by $V_p = (c_{44}/\rho_0)^{1/2}$, where c_{44} (in contracted notation) is the appropriate component of the elastic-stiffness tensor, and ρ_0 is the average mass density of the material. Since the acoustoelectric velocity dispersion is small in the III–V compounds where the electromechanical coupling is weak, it will be neglected in the present investigation. Analyzing the variation of the squared electromechanical coupling constant $\tilde{K}^2(\hat{\kappa}, \hat{\pi})$ with the directions of the acoustic phase propagation ($\hat{\kappa}$) and the polarization, given by the

unit vector $\hat{\pi}$, it is found that the coupling exhibits a maximum for the above mode. Furthermore, the selection rule for the deformation-potential interaction given as $\vec{\Xi} = \hat{\kappa} \cdot \vec{\Xi} \cdot \hat{\pi}$, $\vec{\Xi}$ being the deformation-potential tensor, shows, that this coupling mechanism is forbidden in the present case. We restrict ourselves to scattering geometries which coincide with the (001) plane and assume that the incident light is polarized parallel to the [001] direction (see Fig. 3).

The light scattering from coupled systems of acoustical lattice waves and free-carrier density-waves is generally composed of contributions from (i) the direct photoelastic effect, (ii) the free-carrier screened indirect photoelastic effect, and (iii) the free-carrier-density modulation.[15,16] In the present scattering configuration it follows from the form of the photoelastic, electrooptic, and dielectric tensors that light scattered via (i) and (ii) is polarized in the scattering plane, i.e., changed $\pi/2$ in polarization in relation to the polarization of the unscattered light. A bunching of the free carriers, expressed in terms of the deviation, $n(\vec{r},t)$, of the carrier density from the spatially uniform equilibrium value n_0, causes a quasistatic modulation in the optical dielectric constant given by

$$\vec{\epsilon}^{FC}(\vec{r},t) = \frac{iqn(\vec{r},t)}{\epsilon_0 \omega} \vec{\mu}(\omega)$$

$$= \sum_{\vec{Q}} \vec{\epsilon}_{\vec{Q}}^{FC}(\omega) \exp[i(\vec{Q} \cdot \vec{r} - \Omega_{\vec{Q}} t)] \ , \qquad (52)$$

where $\vec{\mu}(\omega)$ is the free-carrier mobility tensor at the optical frequency. Since the conduction band in indium antimonide has spherically constant-energy surfaces, it follows from Eq. (52) that the light scattered via the conduction-electron bunching has the same direction of polarization as the incident light. The facts mentioned above show that the dynamical diffraction of light by the longitudinal polarized free-carrier-density modulation is not complicated by interference effects with light scattered from the oscillating ions [(i) and (ii)]. It should be realized that the lattice contribution to the scattering, from the present point of view, represents a damping mechanism, which, however, compared to the free-carrier damping is negligible for light frequencies below the plasma frequency. Furthermore, the contribution from the conduction-electron bunching tends to dominate the scattering at low optical frequencies.[13,18,19] The scattering triangle formed by the optical wave vectors is isosceles.

To obtain the scattering from the solid-state plasma one has to calculate the modulation of the free-carrier distribution caused via piezoelectric coupling by a single acoustic mode described by the ionic displacement

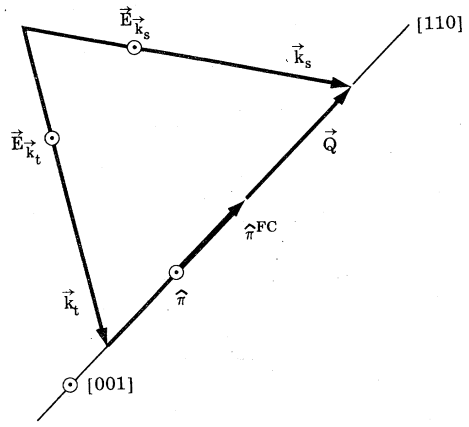

FIG. 3. Schematic diagram showing the diffraction geometry used in the present calculations on n-InSb. The scattering takes place from a longitudinal polarized ($\hat{\pi}^{FC}$) free-carrier-density wave propagating along the [110] direction. The two electromagnetic waves are polarized along the [001] direction. The free-carrier bunching is obtained by coupling to a piezoelectrically active sound wave with polarization along the [001] direction and wave vector along the [110] direction. The scattering plane coincides with the (001) plane.

$$\vec{u}(\vec{r},t) = u_0(\Omega_{\vec{Q}}, \vec{Q}) \hat{\pi} \exp[i(\vec{Q} \cdot \vec{r} - \Omega_{\vec{Q}} t)] \ , \qquad (53)$$

where u_0 is the complex amplitude of the mode. In the following it is assumed that the sound amplitude is sufficiently small that the linear theory of acoustoelectric interaction can be adopted.[37] In turn this means that the bunching of the free carriers in time and space is sinusoidal with an amplitude that increases linearly with the acoustic strain. For the high mobility III–V semiconducting compounds the electron mean-free path can be comparable to or longer than the acoustical wavelength, so that non-local transport effects become significant.[37] Restricting our treatment to acoustic wavelengths which are much larger than the characteristic electron deBroglie wavelength, the response of the electron gas to the acoustic perturbation can be obtained on the basis of a semiclassical Boltzmann-equation calculation of the effective frequency- and wavevector-dependent longitudinal conductivity tensor $\vec{\sigma}_{eff}(\Omega_{\vec{Q}}, \vec{Q})$.[38] For cubic crystals one obtains, by using a drifted Maxwell-Boltzmann distribution for the dc part of the electron distribution and by assuming that an energy-independent momentum relaxation time (τ) approximation can be used, the following scalar expression for the normalized conductivity[39,40]

$$\frac{\tilde{\sigma}_{\text{eff}}(\Omega_{\vec{Q}},\vec{Q})}{\tilde{\sigma}_0}=\frac{-2i(V_p/V_T)Ql[1-\pi^{1/2}wF(w)]}{(Ql)^2[1+2i(1+\gamma)(V_p/V_T)(Ql)^{-1}][1-\pi^{1/2}uF(u)(1-i(V_p/V_T)Ql)]}\ , \tag{54}$$

with

$$u=\frac{1-i\frac{V_p}{V_T}Ql}{Ql\left[1+2i(1+\gamma)\frac{V_p}{V_T}(Ql)^{-1}\right]^{1/2}}\ , \tag{55}$$

$$w=\frac{1+i\gamma\frac{V_p}{V_T}Ql}{Ql\left[1+2i(1+\gamma)\frac{V_p}{V_T}(Ql)^{-1}\right]^{1/2}}\ , \tag{56}$$

and with the real and imaginary part of F given by the integral representations[41]

$$\mathrm{Re}F(x+iy)=\frac{1}{\pi}\int_{-\infty}^{\infty}\frac{x\exp(-t^2)}{x^2+(y+t)^2}dt\ ,\quad x>0\ , \tag{57}$$

$$\mathrm{Im}F(x+iy)=-\frac{1}{\pi}\int_{-\infty}^{\infty}\frac{(y+t)\exp(-t^2)}{x^2+(y+t)^2}dt\ . \tag{58}$$

In the set of Eqs. (54)–(58), $\tilde{\sigma}_0=qn_0\tilde{\mu}_0$ denotes the dc conductivity, $\gamma=V_d/V_p-1$ is the drift parameter (V_d being the drift velocity of the free carriers), $V_T=(2k_BT/\tilde{m}^*)^{1/2}$ is the thermal electron velocity, and $l=V_T\tau$ is the electron mean-free path. The dc mobility and the effective mass of the carriers are named $\tilde{\mu}_0$ and $\tilde{m}^*$. It is apparent from Eqs. (54)–(58) that $\tilde{\sigma}_{\text{eff}}/\tilde{\sigma}_0$ depends on the three dimensionless parameters Ql, γ, and V_p/V_T only. To evaluate $\tilde{\sigma}_{\text{eff}}/\tilde{\sigma}_0$ as a function of $\Omega_{\vec{Q}}\tau$ one has to make the replacement $Ql=(V_T/V_p)\,\Omega_{\vec{Q}}\tau$.

On the basis of $\tilde{\sigma}_{\text{eff}}/\tilde{\sigma}_0$ the free-carrier-density modulation $\tilde{\Delta}_{\vec{Q}}=n_{\vec{Q}}/n_0$, giving the ratio between the amplitude ($n_{\vec{Q}}$) of the space-charge-density wave and the thermal equilibirum density (n_0), takes (numerically) the form[15,16]

$$|\tilde{\Delta}_{\vec{Q}}|=\left(\frac{2\rho_0}{V}\right)^{1/2}\frac{\tilde{e}\tilde{\mu}_0}{\tilde{c}\tilde{\epsilon}_0^s\epsilon_0}\left(\frac{I}{I_{\text{th}}}\right)^{1/2}\left[\frac{\hbar\Omega_{\vec{Q}}}{\exp(\hbar\Omega_{\vec{Q}}/k_BT)-1}\right]^{1/2}\frac{|\tilde{\sigma}_{\text{eff}}/\tilde{\sigma}_0|}{|1+i(\tilde{\sigma}_{\text{eff}}/\tilde{\sigma}_0)(\tilde{\Omega}_c/\Omega_{\vec{Q}})|}\ , \tag{59}$$

where V is the normalization volume for the lattice modes and $\tilde{\epsilon}_0^s$, $\tilde{e}$, $\tilde{c}$, and $\tilde{\Omega}_c=\tilde{\sigma}_0/\epsilon_0^s\epsilon_0$ are the appropriate relative static dielectric constant, piezoelectric constant, elastic-stiffness constant, and conductivity relaxation frequency, and I/I_{th} is the acoustic intensity (I) relative to the thermal equilibrium intensity (I_{th}) of the mode.

For a parabolic band structure the appropriate optical, low-field relative dielectric constant can be written on the form[20,36]

$$\tilde{\epsilon}_0=\tilde{\epsilon}_0^L\left[1+\frac{\tilde{\omega}_p^2\tau}{\omega}\frac{i-\omega\tau}{1+(\omega\tau)^2}\right]\ , \tag{60}$$

in the energy-independent electron relaxation time approximation. It follows from Eq. (60) that the perturbation of $\tilde{\epsilon}_0$ caused by the space-charge density wave numerically is given by

$$|\tilde{\epsilon}_{\vec{Q}}|=\tilde{\epsilon}_0^L\frac{\tilde{\omega}_p^2\tau}{\omega}[1+(\omega\tau)^2]^{-1/2}|\tilde{\Delta}_{\vec{Q}}|\ . \tag{61}$$

Equation (61) completes the set of formulas which allow us to calculate, in the linear regime of acoustoelectric coupling, the complex wave vector components $k^{\pm}$, $\gamma^{\pm}$, and the reflectivity $|R_{\perp}|^2$ as a function of one of the dimensionless "external" parameters $\Omega_{\vec{Q}}\tau$, $\omega\tau$, γ, V_p/V_T, or I/I_{th}.

B. Anomalous transmission in the collision-dominated regime ($Ql \ll 1$) of acoustoelectric interaction

To fulfill the phase matching condition on the scattering kinematics given in Eq. (9) one must restrict the ranges of acoustical and optical frequencies by the inequality

$$\omega/c\geq\frac{\Omega_{\vec{Q}}}{2V_p}\ . \tag{62}$$

The frequency of maximum acoustoelectric gain is given by $\tilde{\Omega}_m=(\tilde{\Omega}_c\tilde{\Omega}_D)^{1/2}$ for the collision-dominated electron gas ($Ql\ll 1$) and by $\sqrt{3}\,\tilde{\Omega}_m$ for the collisionless gas ($Ql\gg 1$), $\tilde{\Omega}_D=(qV_p^2/\tilde{\mu}_0k_BT)^{1/2}$ denoting the appropriate free-carrier diffusion frequency. Writing $\tilde{\Omega}_m$ in the form

$$\tilde{\Omega}_m=\sqrt{2}(V_p/V_T)\tilde{\omega}_p\ , \tag{63}$$

the condition in Eq. (62) can be expressed as follows

$$\frac{\Omega_{\vec{Q}}}{\tilde{\Omega}_m}\leq\sqrt{2}\frac{V_T}{c}\frac{\omega}{\tilde{\omega}_p}\ . \tag{64}$$

Since the treatment in Sec. VIII A holds in the nonrelativistic range of conduction electron velocities only, and moreover since for practical temperatures

$V_T/c \leq 10^{-2}$ it follows from Eq. (64) that one has $\Omega_{\vec{Q}}/\tilde{\Omega}_m \leq 10^{-2}$ for optical frequencies around and below the plasma frequency. This in turn shows that the macroscopic Hutson-White theory of acoustoelectric interaction can be applied when calculating $|\tilde{\Delta}_{\vec{Q}}|$ for $\omega/\tilde{\omega}_p \leq 10$, an optical frequency range which should be of primary interest for experimental investigations of sound induced anomalous transmission effects in the III–V compounds.

In the collision-dominated region of acoustoelectric coupling the normalized effective conductivity is reduced to

$$\frac{\tilde{\sigma}_{\text{eff}}}{\tilde{\sigma}_0} = \left[\gamma + i\frac{\Omega_{\vec{Q}}}{\tilde{\Omega}_D}\right]^{-1}, \quad Ql \ll 1 \ , \tag{65}$$

which implies that the free-carrier modulation becomes

$$|\tilde{\Delta}_{\vec{Q}}| = \left(\frac{2\rho_0}{V}\right)^{1/2} \frac{\tilde{e}\tilde{\mu}_0}{\tilde{c}\tilde{\epsilon}_0^s \epsilon_0} \left(\frac{I}{I_{\text{th}}}\right)^{1/2} \times \left(\frac{\hbar\Omega_{\vec{Q}}}{\exp(\hbar\Omega_{\vec{Q}}/k_B T) - 1}\right)^{1/2} \times \left[\gamma^2 + \frac{\tilde{\Omega}_c}{\tilde{\Omega}_D}\left(\frac{\tilde{\Omega}_m}{\Omega_{\vec{Q}}} + \frac{\Omega_{\vec{Q}}}{\tilde{\Omega}_m}\right)^2\right]^{-1/2} ,$$

$$Ql \ll 1 \ . \tag{66}$$

Let us now consider microwave sound at not too low temperatures so that $\hbar\Omega_{\vec{Q}} \ll k_B T$, and let us introduce the approximation $\gamma^2 \leq \tilde{\Omega}_c/\tilde{\Omega}_D$, which usually is correct in the high-conductivity limit applicable to semiconducting materials. Utilizing that $\Omega_{\vec{Q}} \ll \tilde{\Omega}_m$ the charge-density modulation now takes a form

$$|\tilde{\Delta}_{\vec{Q}}| = V^{-1/2} \frac{\tilde{K}}{n_0^{1/2}} \frac{V_T}{V_p} \left(\frac{I}{I_{\text{th}}}\right)^{1/2} \frac{\Omega_{\vec{Q}}}{\tilde{\omega}_p} \left(\frac{\tilde{\epsilon}_0^s}{\tilde{\epsilon}_0^L}\right)^{1/2} , \tag{67}$$

where $\tilde{K} = (\tilde{e}^2/\tilde{c}\tilde{\epsilon}_0^s\epsilon_0)^{1/2}$. Equation (67) indicates that $|\tilde{\Delta}_{\vec{Q}}|$ increases linearly as a function of $\Omega_{\vec{Q}}$.

If the solid-state plasma from an "optical" point of view is collisionless ($\omega\tau \gg 1$) it follows by combining Eqs. (43) and (67) that the amplitude attenuation coefficients are given by

$$\gamma^{\pm} = \frac{\tilde{\omega}_p}{c/(\tilde{\epsilon}_0^L)^{1/2}} \left[\left(\frac{c/(\tilde{\epsilon}_0^L)^{1/2}}{2V_p}\right)^2 \left(\frac{\Omega_{\vec{Q}}}{\tilde{\omega}_p}\right)^2 \mp \frac{\tilde{K}}{(Vn_0)^{1/2}} \frac{V_T}{V_p} \left(\frac{I}{I_{\text{th}}}\right)^{1/2} \frac{\Omega_{\vec{Q}}}{\tilde{\omega}_p} \left(\frac{\epsilon_0^s}{\tilde{\epsilon}_0^L}\right)^{1/2} + 1 - \left(\frac{\omega}{\tilde{\omega}_p}\right)^2\right]^{1/2} , \omega\tau \gg 1 \ , \tag{68}$$

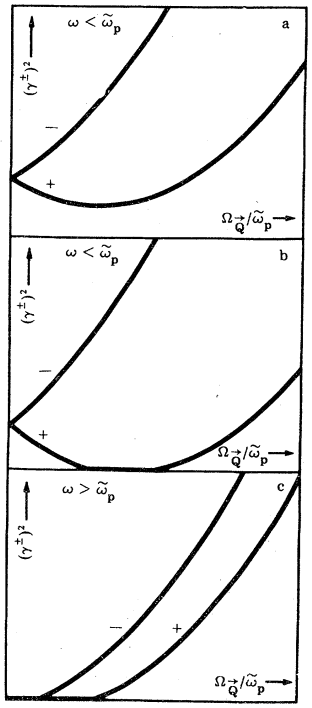

FIG. 4. Schematic diagrams showing the squared amplitude attenuation coefficients of the two eigenmodes as functions of a reduced acoustical frequency. Figures 4(a) and 4(b) correspond to "high" and "low" free-carrier modulation, respectively. The optical frequency is smaller than the plasma frequency. In Fig. 4(c) is $\omega > \tilde{\omega}_p$.

for $\omega \geq \tilde{\omega}_{\text{dyn}}^{\pm}$. To analyze the attenuation coefficients as functions of the acoustical frequency, we have plotted schematically $(\gamma^{\pm})^2$ as functions of $\Omega/\tilde{\omega}_p$ in Fig. 4. Parts (a) and (b) of the figure correspond to $\omega < \tilde{\omega}_p$, and part (c) to $\omega > \tilde{\omega}_p$. In all plots $(\gamma^{\pm})^2$ and $(\gamma^-)^2$ are parabolic functions of $\Omega_{\vec{Q}}/\tilde{\omega}_p$.

In Fig. 4(a) the degree of free-carrier modulation is so low that no zeros occur for the damping of the plus-sign mode. The attenuation of the minus-sign mode increases monotonically as a function of $\Omega_{\vec{Q}}/\tilde{\omega}_p$, whereas the attenuation of the plus-sign mode passes through a minimum

$$\gamma_{\text{min}}^{+} = \frac{\tilde{\omega}_p}{c/(\tilde{\epsilon}_0^L)^{1/2}} \left[1 - \left(\frac{\omega}{\tilde{\omega}_p}\right)^2 - \frac{\tilde{K}^2}{Vn_0}\left(\frac{V_T}{c/(\tilde{\epsilon}_0^L)^{1/2}}\right)^2 \frac{I}{I_{\text{th}}} \frac{\tilde{\epsilon}_0^s}{\tilde{\epsilon}_0^L}\right]^{1/2} \tag{69}$$

at $\Omega_{\vec{Q}}/\tilde{\omega}_p = 2[\tilde{K}/(Vn_0)^{1/2}]\{V_p V_T/[c/(\tilde{\epsilon}_0^L)^{1/2}]^2\}(I/I_{\text{th}})^{1/2} \times (\tilde{\epsilon}_0^s/\tilde{\epsilon}_0^L)^{1/2}$. For $\Omega_{\vec{Q}}/\tilde{\omega}_p \to 0$, γ^+ and γ^- both approach the unperturbed attenuation

$\gamma^0 = (\tilde{\omega}_p^2 - \omega^2)^{1/2}/[c/(\tilde{\epsilon}_0^L)^{1/2}]$. It is apparent that γ^+ is less than γ^0 for normalized acoustic frequencies in the range $0 < \Omega_{\vec{Q}}/\tilde{\omega}_p < 4[\tilde{K}/(Vn_0)^{1/2}] \times \{V_p V_T/[c/(\tilde{\epsilon}_0^L)^{1/2}]^2\}(I/I_{\text{th}})^{1/2}\,(\tilde{\epsilon}_0^s/\tilde{\epsilon}_0^L)^{1/2}$.

In Fig. 4(b) the degree of free-carrier modulation is so high that the attenuation of the plus-sign mode goes to zero in a certain range of acoustical frequencies, indicating the occurrence of a frequency band of perfect anomalous transmission. Note that the condition for obtaining an exact zero of γ^+ is that $\omega\tau \to \infty$. In a realistic calculation (see Sec. VIII C) a small attenuation arising from the imaginary part of $\tilde{\epsilon}_0$ remains.

For the higher acoustical frequencies both γ^+ and γ^- are larger than γ^0. This is due to the fact that the scattering angles θ_t^+ and θ_t^- (disregarding boundary refraction) approach $\pi/2$ for increasing $\Omega_{\vec{Q}}$, thereby increasing the attenuation parallel to the acoustical wave fronts towards infinity [see Eq. (34)].

The distinction between "high" and "low" free-carrier modulation is made on basis of inequality

$$\frac{2\tilde{K}^2 W}{\tilde{\omega}_p^2 - \omega^2} > \epsilon_0 c^2 \left(\frac{\tilde{m}^*}{q}\right)^2 \left(\frac{\tilde{\epsilon}_0^L}{\tilde{\epsilon}_0^s}\right), \tag{70}$$

where W is the acoustical energy density of the mode in consideration. If the inequality holds we are in the "high"-modulation region, else in the "low"-modulation region.

In Fig. 4(c), γ^0 is zero since $\omega > \tilde{\omega}_p$. With regard to the plus- and minus-sign branch the increase in scattering angles with $\Omega_{\vec{Q}}/\tilde{\omega}_p$ causes finite, monotonically increasing attenuation coefficients above certain acoustic frequencies as shown.

It should be pointed out that the phase matching condition in Eq. (62) sets an upper limit, $\Omega_{\vec{Q}}/\tilde{\omega}_p < 2(V_p/c)(\omega/\tilde{\omega}_p)$ on the accessible frequency range. This we shall see more explicitly below.

C. Numerical results

In order to obtain significant dynamical diffraction effects the degree of free-carrier bunching ($\tilde{\Delta}_{\vec{Q}}$) should be high, yet for the present work with the restriction imposed by our use of the linear theory of acoustoelectric coupling.[37] In a forthcoming paper we shall undertake a study of dynamical light diffraction in strong piezoelectric semiconductors like ZnO and CdS in the case where nonlinear free-carrier bunching effects are of importance. To achieve a large degree of free-carrier modulation in a weak piezoelectric crystal like InSb one has to use (i) samples of very low free-carrier densities and (ii) large sound intensities. In the following numerical results for InSb crystals having an excess n-type carrier density $n_0 = 3 \times 10^{19}$ m^{-3} and a corresponding Hall mobility $\tilde{\mu}_0 = 1.2 \times 10^2$ m^2/V sec at $T = 80$ K are presented. Indium antimonide crystals with approximately the above specifications can be produced by extensive purification followed by controlled crystal growth.[42] The remaining data used in the calculations are: $V_p^L = 2.3 \times 10^3$ m/sec,[37] $e_{14} = 0.071$, C/m^2,[43] $\tilde{\epsilon}_0^L = 15.7$,[44] $\tilde{\epsilon}_0^s = 17.8$,[44] $\tilde{K}^2 = 1.2 \times 10^{-3}$,[45] and $\tilde{m}^*/m_0 = 0.014$.[46] As derivatives of the above data we take $\tau = \tilde{\mu}_0 \tilde{m}^*/q$, $c_{44} = e_{14}^2/\tilde{K}^2 \tilde{\epsilon}_0^s \epsilon_0$, $\rho_0 = c_{44}/V_p^2$, and $\tilde{\omega}_p = (n_0 q^2/\tilde{\epsilon}_0^L \epsilon_0 \tilde{m}^*)^{1/2}$. As dimensionless "external" parameters in the calculations we have the quantities I/I_{th}, γ, $\Omega_{\vec{Q}}\tau$, and $\omega/\tilde{\omega}_p$. Referring the numerical results below to a unit volume of normalization ($V = 1$ m^3) for the lattice modes, the thermal intensity I_{th} approximates $I_{\text{th}} \cong (kT/V)V_p \cong 2.5 \times 10^{-18}$ W/m^2 for $\hbar\Omega_{\vec{Q}} \ll k_B T$. Thus choosing $I/I_{\text{th}} = 10^{25}$ implies that the acoustical intensity in our calculations is $I \cong 2.5$ kW/cm^2. The peak shear strain corresponding to this mode intensity is as high as 9.0×10^{-4}. It appears from the approximate formula given in Eq. (67) that the free-carrier bunching is almost independent of the drift parameter in the present case. This is confirmed by detailed numerical calculations based on the complete expression for $|\tilde{\Delta}_{\vec{Q}}|$ [Eq. (59)].

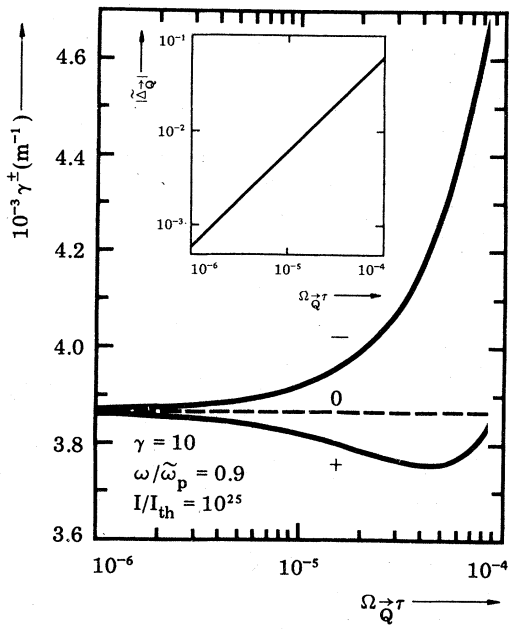

FIG. 5. Amplitude attenuation coefficients of the two eigenmodes (+, −) as functions of a dimensionless acoustical frequency with selected values for the "external" parameters: the optical frequency, the drift parameter, and the sound intensity. For comparison it is shown the attenuation coefficient (0) corresponding to unperturbed wave propagation. The upper cutoff is at $\Omega_{\vec{Q}}\tau \cong 8.6 \times 10^{-4}$. The material data are given in the text. The insert shows the degree of free-carrier modulation as a function of the (dimensionless) acoustical frequency.

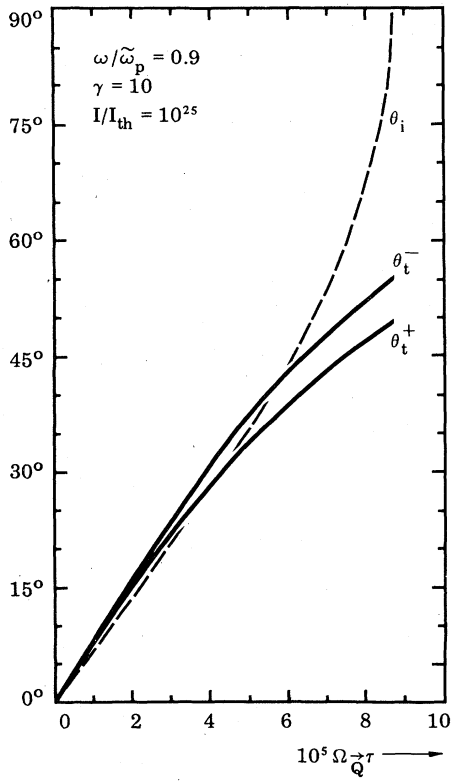

FIG. 6. Bragg angle (θ_i) outside the crystal, and angles of dynamical refraction (θ_t^+, θ_t^-) as functions of a dimensionless acoustical frequency. The upper cutoff is at $\Omega_{\vec{Q}}\tau \cong 8.6 \times 10^{-4}$. The parameter values and the material data are as in Fig. 5.

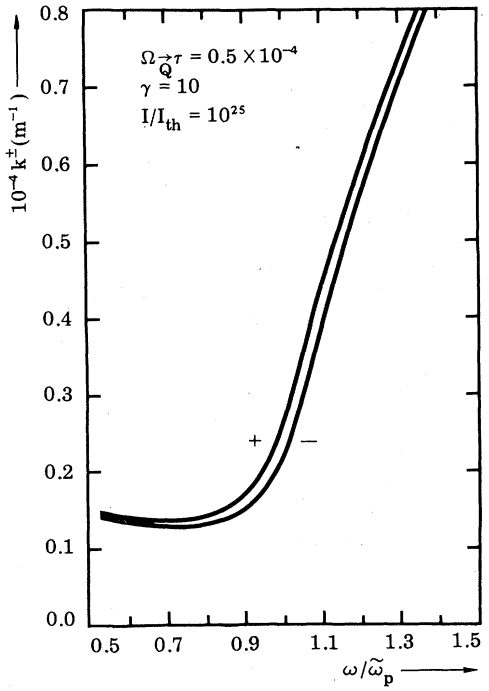

FIG. 7. Dispersion relations for the dynamically diffracted eigenmodes (+, −) for selected values of the (dimensionless) acoustical frequency, the drift parameter, and the sound intensity. The material data are given in the text.

Below we shall always take $\gamma = 10$.[45] The following calculations are all made using the complete set of Eqs. (15), (16), (24), and (54)–(61).

In Fig. 5 is shown γ^+ and γ^- as functions of the dimensionless acoustical frequency $\Omega_{\vec{Q}}\tau$ at an optical frequency $\omega = 0.9\tilde{\omega}_p$. For comparison is plotted the attenuation coefficient (γ^0) for unperturbed wave propagation perpendicular to the surface. The upper limit for $\Omega_{\vec{Q}}\tau$, given by the phase matching condition in Eq. (62), is $\sim 8.6 \times 10^{-4}$. The inequality in (70) shows that we are in the "low"-modulation region, and in accordance with this the plus-sign mode passes through a minimum. The insert of Fig. 5 shows $|\tilde{\Delta}_{\vec{Q}}|$ as a function of $\Omega_{\vec{Q}}\tau$. As expected from Eq. (67) the bunching increases linearly as a function of the acoustical frequency. Furthermore, the free-carrier modulation is small ($|\tilde{\Delta}_{\vec{Q}}| \leq 5 \times 10^{-2}$) in the accessible acoustical frequency range. The Bragg angle (θ_i) outside the crystal, and the angles of refraction θ_t^+ and θ_t^- for the eigenmodes are shown as functions of the dimensionless acoustical frequency in Fig. 6. Note that one always has $\theta_t^- > \theta_t^+$, whereas one can have $\theta_i < \theta_t^+$, $\theta_t^+ < \theta_i < \theta_t^-$, or $\theta_i > \theta_t^-$.

The dispersion relations $[k^{\pm}(\omega/\tilde{\omega}_p)]$ for the plus- and minus-sign modes have been calculated for a parameter value $\Omega_{\vec{Q}}\tau = 0.5 \times 10^{-4}$. The results are shown in Fig. 7. For optical frequencies $\omega \gtrsim \tilde{\omega}_p$ the propagation constants and the splitting of the plasma dispersion relation follows closely the predictions based on the theory of dynamical light diffraction in a collisionless ($\omega\tau >> 1$) electron gas [see Eq. (40)]. For frequencies above the lower cutoff frequency $\omega \cong 0.53\tilde{\omega}_p$ and below $\sim\tilde{\omega}_p$ the contributions from the imaginary part of $\tilde{\epsilon}_0$ tends to determine the shape of the branches of the dispersion relation. The attenuation coefficients γ^+ and γ^-, corresponding to the propagation constants of Fig. 7, are shown, as functions of the normalized optical frequency $\omega/\tilde{\omega}_p$, in Fig. 8. Below the plasma frequency the attenuation coefficients, and thus the splitting of the unperturbed attenuation coefficient, are determined mainly by the simplified expression in Eq. (68). Above the

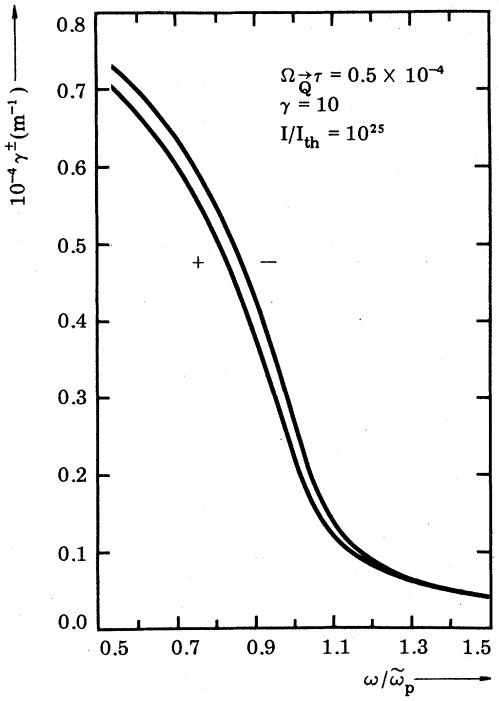

FIG. 8. Amplitude attenuation coefficients for the dynamically diffracted eigenmodes (+, −) as functions of a normalized optical frequency. "External" parameters and material data are as in Fig. 7.

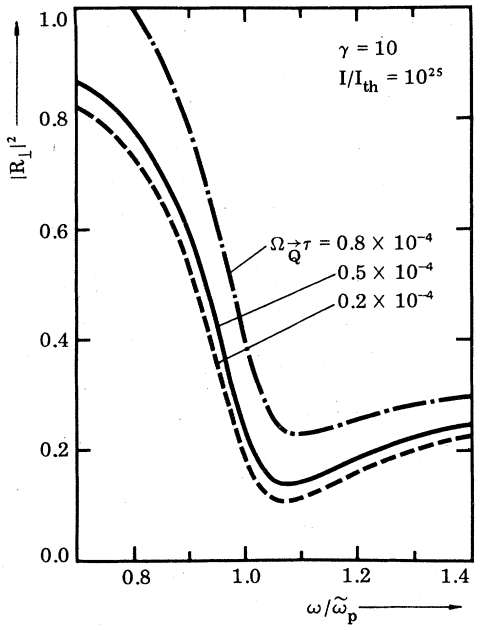

FIG. 9. Reflectance as a function of a normalized optical frequency with the (dimensionless) acoustical frequency as a parameter. The material data are identical to those of Fig. 7.

plasma edge γ^+ and γ^- tend to coincide for increasing ω.

The reflectance $|R_\perp|^2$ calculated as a function of $\omega/\tilde{\omega}_p$ is shown in Fig. 9 for three values of $\Omega_{\vec{Q}}\tau$. With the vertical scale used in this figure the reflectance for $\Omega_{\vec{Q}}\tau = 0.2 \times 10^{-4}$ coincides with that obtained for incidence on a crystal in the limit of spatially uniform free-carrier density.

IX. CONCLUDING REMARKS

The Borrmann effect for x rays, neutrons, and electrons originates in the interference of the incident and Bragg scattered parts of the wave field. Since it is a necessary condition for Bragg diffraction that, roughly speaking, the wavelength of the incoming radiation is smaller than the spacing of the set of scattering lattice planes, anomalous transmission of infrared, visible or ultraviolet light through strongly absorbing crystals by natural dynamical diffraction is impossible. However, as pointed out by the present author, it should be possible to obtain a significant induced Borrmann effect for light by creating a spatial periodicity in the free-carrier density matching optical wavelengths. The present theoretical work on *n*-InSb shows that the possibilities for observing induced anomalous transmission of light through piezoelectric semiconductors below the plasma edge by modulating the free-carrier distribution by an acoustical wave via the piezoelectric coupling are promising even in weak piezoelectric III–V semiconductors. Work on strong piezoelectric II–VI compounds like ZnO and CdS are in progress. Preliminary results for these noncubic crystals show possibilities for a dramatic reduction of the attenuation of electromagnetic waves below the plasma edge.

[1]M. Cardona *et al.*, *Light Scattering in Solids, Topics in Applied Physics* (Springer-Verlag, Berlin, 1975), Vol. 8.

[2]*Proceedings of the Third International Conference on Light Scattering in Solids,* edited by M. Balkanski, R. C. C. Leite, and S. P. S. Porto (Flammarion, Paris, 1975).

[3]F. Pöckels, Ann. Phys. (Leipzig.) 37, 144 (1889); 37, 269 (1889); 37, 372 (1889); 39, 440 (1890).

[4]M. Born and K. Huang, *Dynamical Theory of Crystal Lattices*

(Clarendon, Oxford, 1954).
[5]G. B. Benedek and K. Fritsch, Phys. Rev. 149, 647 (1966).
[6]D. F. Nelson and M. Lax, Phys. Rev. Lett. 24, 379 (1970).
[7]J. Chapelle and L. Taurel, C. R. Acad. Sci. (Paris) 240, 743 (1955).
[8]D. F. Nelson and M. Lax, Phys. Rev. B 3, 2778 (1971).
[9]R. Loudon, Proc. R. Soc. A 275, 218 (1963).
[10]E. Burstein, R. Ito, A. Pinczuk, and M. Shand, J. Acoust. Soc. Am. 49, 1013 (1971).
[11]W. Brening, R. Zeyher, and J. L. Birman, Phys. Rev. 36, 4617 (1972).
[12]*Polaritons,* edited by E. Burstein and F. De Martini (Pergamon, New York, 1974).
[13]O. Keller, in *Proceedings of the Third International Conference on Light Scattering in Solids,* edited by M. Balkanski, R. C. C. Leite, and S. P. S. Porto (Flammarion, Paris, 1975), p. 477.
[14]O. Keller, Solid State Commun. 18, 1227 (1976).
[15]O. Keller, Phys. Rev. B 13, 4612 (1976).
[16]O. Keller, Spectrosc. Lett. 9, 545 (1976).
[17]P. M. Platzman and P. A. Wolff, Solid State Phys. Suppl. 13, 1 (1973).
[18]V. V. Proklov, G. N. Shkerdin, and Yu. V. Gulyaev, Solid State Commun. 10, 1145 (1972).
[19]V. V. Proklov, G. N. Shkerdin, and Yu. V. Gulyaev, Sov. Phys.-Semicond. 6, 1646 (1973).
[20]O. Keller, J. Opt. Soc. Am. 68, 42 (1978).
[21]D. L. Mills, A. A. Maradudin, and E. Burstein, Ann. Phys. (N. Y.) 56, 504 (1970).
[22]R. Zeyher, C. S. Ting, and J. L. Birman, Phys. Rev. B 10, 1725 (1974).
[23]G. Borrmann, Z. Phys. 127, 297 (1950).
[24]J. P. Hannon and G. T. Trammell, Phys. Rev. 186, 306 (1969).
[25]B. W. Batterman and H. Cole, Rev. Mod. Phys. 36, 681 (1964).
[26]M. Ashkin and M. Kuriyama, J. Phys. Soc. Jpn. 21, 1549 (1966).
[27]M. Kuriyama, Acta Crystallogr. A 31, 774 (1975).
[28]A. M. Afanas'ev and Yu. Kagan, Acta Crystallogr. A 24, 163 (1967).
[29]D. A. O'Connor, Proc. Phys. Soc. 91, 917 (1967).
[30]C. R. Hall and P. B. Hirsch, Proc. R. Soc. A 286, 158 (1964).
[31]O. Keller, Spectrosc. Lett. 11, 187 (1978).
[32]O. Keller and C. Søndergaard, Jpn. J. Appl. Phys. 13, 1765 (1974).
[33]J. D. Gil and E. M. Brady, in Ref. 13.
[34]G. Dresselhaus and A. S. Pine, Solid State Commun. 16, 1001 (1975).
[35]D. Pines, *Elementary Excitations in Solids,* (Benjamin, New York, 1963).
[36]C. Herring, Bell Syst. Tech. J. 34, 237 (1955).
[37]H. Kuzmany, Phys. Status Solidi A 25, 9 (1974).
[38]H. N. Spector, Solid State Phys. 19, 291 (1966).
[39]H. N. Spector, Phys. Rev. 165, 562 (1968).
[40]E. Mosekilde, D. Sc. thesis, (University of Copenhagen, 1977) (unpublished).
[41]*Handbook of Mathematical Functions,* edited by M. Abramovitz and I. A. Stegun, Natl. Bur. of Stand. Appl. Math. Ser. No. 55 (U. S. GPO, Washington, D. C., 1967), pp. 297–328.
[42]S. G. Parker, O. W. Wilson, and B. H. Barbee, J. Electrochem. Soc. 112, 80 (1965).
[43]G. Arlt and P. Quadfleig, Phys. Status Solidi 25, 233 (1968).
[44]M. Neuberger, *Handbook of Electronic Materials,* (IFI/Plenum, New York, 1971), Vol. 2, p. 77.
[45]R. Route, M. L. Report No. 1817 (Stanford University, 1970) (unpublished).
[46]W. G. Spitzer and H. Y. Fan, Phys. Rev. 106, 882 (1957).

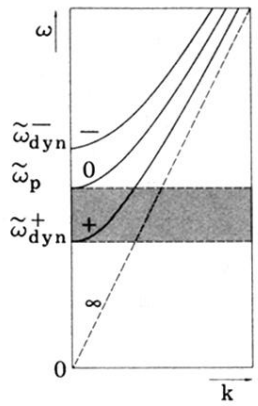

FIG. 2. Dispersion relations for dynamically diffracted (+, −) and undiffracted (0) electromagnetic eigenmodes of long wavelength in a collisionless solid-state plasma. Neglecting band-structure effects the curves approach a common nondispersive $\omega(\vec{k})$ relation (∞) at high frequencies. In the shaded region anomalous transmission takes place for the plus-sign mode.